Accepted Manuscript

Discovery and structure-activity-relationship study of novel conformationally restricted indane analogues for mutant isocitric dehydrogenase 1 (IDH1) inhibitors

Qiangang Zheng, Shuai tang, Xianlei Fu, Ziqi Chen, Yan Ye, Xiaojing Lan, Lei Jiang, Ying Huang, Jian Ding, Meiyu Geng, Min Huang, Huixin Wan

PII: S0960-894X(17)31014-4
DOI: https://doi.org/10.1016/j.bmcl.2017.10.029
Reference: BMCL 25358

To appear in: *Bioorganic & Medicinal Chemistry Letters*

Received Date: 29 August 2017
Revised Date: 13 October 2017
Accepted Date: 14 October 2017

Please cite this article as: Zheng, Q., tang, S., Fu, X., Chen, Z., Ye, Y., Lan, X., Jiang, L., Huang, Y., Ding, J., Geng, M., Huang, M., Wan, H., Discovery and structure-activity-relationship study of novel conformationally restricted indane analogues for mutant isocitric dehydrogenase 1 (IDH1) inhibitors, *Bioorganic & Medicinal Chemistry Letters* (2017), doi: https://doi.org/10.1016/j.bmcl.2017.10.029

Graphical Abstract

To create your abstract, type over the instructions in the template box below.
Fonts or abstract dimensions should not be changed or altered.

Discovery and structure-activity-relationship study of novel conformationally restricted indane analogues for mutant isocitric dehydrogenase 1 (IDH1) inhibitors

Leave this area blank for abstract info.

Qiangang Zheng[a,#] , *Shuai Tang*[b,#], *Xianlei Fu*[a] , *Ziqi Chen*[b] , *Yan Ye*[a,b], *Xiaojing Lan*[b], *Lei Jiang*[a] ,*Ying Huang*[a], *Jian Ding*[b] , *MeiyuGeng*[b] , *Min Huang* [b],*,*Huixin Wan* [a,*]

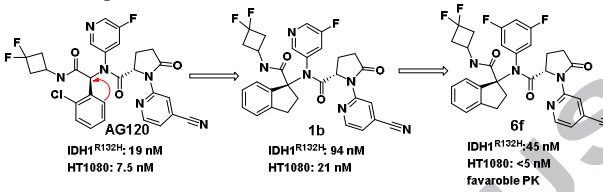

Bioorganic & Medicinal Chemistry Letters
journal homepage: www.elsevier.com

Discovery and structure-activity-relationship study of novel conformationally restricted indane analogues for mutant isocitric dehydrogenase 1 (IDH1) inhibitors

Qiangang Zheng[a,#] , Shuai tang[b,#], Xianlei Fu[a] , Ziqi Chen[b], Yan Ye[a,b] , Xiaojing Lan[b], Lei Jiang[a], Ying Huang[a], Jian Ding[b] , MeiyuGeng[b] , Min Huang[b,*], Huixin Wan[a,*]

[a] *Shanghai Haihe Pharmaceutical, Co.,Ltd. 421 Newton Road, Zhangjiang Hi-tech Park, Pudong New Area, Shanghai, 201203,China*

[b] *Shanghai Institute of Materia Medica, Chinese Academy of Science, 555 Zuchongzhi Road, Zhangjiang Hi-tech Park, Pudong New Area, Shanghai, 201203, China*

#, these authors contributed equally to this work.

*, corresponding authors.

ARTICLE INFO

Article history:
Received
Revised
Accepted
Available online

Keywords:
IDH1 inhibitor
indane amide
structure-based rational design

ABSTRACT

The discovery and optimization of various of indane amides as mutant IDH1 inhibitors *via* structure-based rational design were reported. The optimal compounds demonstrated both potent inhibition in IDH1^{R132H} enzymatic activity and 2HG production in IDH1 mutant HT1080 cell line, favorable PK properties and great selectivity against IDH1^{wt} and IDH2 ^{R140Q}.

Isocitrate dehydrogenase family, including IDH1, IDH2 and IDH3, are important metabolic enzymes, that can convert isocitrate to α-ketoglutarate (α-KG). Somatic cancer-associated IDH mutations have been identified in multiple hematologic and solid tumors, such as acute myeloid leukemia (AML),[1] glioma,[2] cholangiocarcinoma cancer (IHCC),[3] malignant chondrosarcomas[4] and others.[5] IDH mutations often occur at R132 in IDH1 or R140 and R172 in IDH2, which are located in the catalytic pocket of these enzymes. Significantly, these mutations allow IDH enzymes to gain a unique activity, that catalytically converts α-KG to an onco-metabolite 2-hydroxyglutarate (2-HG). The onco-metabolite (2-HG) is strongly associated to impaired hematopoietic differentiation and promotes leukemia due to its ability of global DNA hypermethylation.[6] Pharmacological blockade of mutant IDH1 enzyme effectively inhibits colony formation of patient-derived IDH-mutated AML cells but not that of normal CD34+ bone marrow cells.[7] As such, mutant IDH has now become a therapeutic target of great interest for cancer, especially AML, although the contribution of mutant IDH to tumorigenic properties remains to be elucidated.

Mutant IDH has now become a therapeutic target of great interest in the field of antitumor drug discovery, and several big pharmaceutical companies and new start-ups have paid much more attention to discovery and development of mutant IDH inhibitors. AG120 is one of the most advanced compound entered into clinical trials as a mutant IDH1 inhibitor discovered by Agios and has shown promising clinical benefit with 38% overall response rate for advanced hematologic malignancies. [8] This compound contains a metabolic labile amide bond and two epimerizable tertiary centers. In light of these, we proposed a novel conformationally restricted scaffold with a quaternary center at the backbone of AG120 (**Figure 1**).

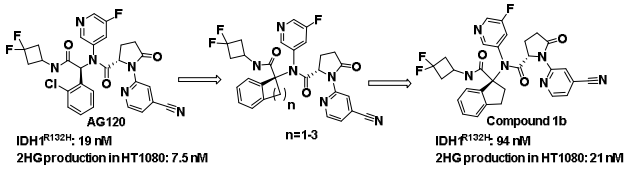

Figure 1. From AG120 to the indane analogue compound **1b**.

The installation of a quaternary center at α-position of amide would prevent epimerization and potentially slow down amide hydrolysis. Among these fused rings shown in **Table 1**, the indane analogue **1b** retained most of the biochemical and cellular activities of AG120. Compound **1b** showed moderate activities in both IDH1^{R132H} enzymatic assay (IC_{50}=94 nM) and the 2-HG production inhibitory assay in HT1080 (IC_{50}=21 nM), a human sarcoma cell line carrying mutant IDH1. It was a very

encouraging start point for us to improve the in vitro potency of this series of indane analogues.

Table 1. Enzymatic inhibition activities of different fused ring analogues **1a**-**1c**.

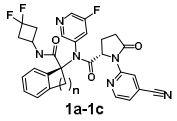

Cmpd	n	IDH1^{R132H} IC_{50} (nM)	2-HG HT1080 [a] IC_{50}(nM)
1a	1	270	NT
1b	2	94	21
1c	3	275	NT

a, Compounds with IDH1^{R132H} IC_{50} <100 nM was tested against 2-HG production inhibitions on HT1080. NT, means not test.

Encouraged by these results, herein we would describe the discovery, optimization and SAR studies of a novel conformationally restricted indane analogues as mutant IDH1 inhibitors. A multi-step approach to synthesize the designed compounds would involve three key steps (**Scheme 1**): (a) Indanone and aromatic amine containing UGI reaction; [9] (b) Buchwald-Hartwig coupling with amide-NH and haloaromatic ring; (c) Separation of diastereomers on HPLC or flash chromatography. [10] When X is CH, a four components UGI reaction afforded the indane amide backbone, subsequently a Buchwald-Hartwig cross coupling reaction was followed with diastereomers isolation from moderate to high yields. However, when X is N, classical UGI conditions (step a, **Scheme 1**) by mixing all the components in dried MeOH did not proceed well with recovery of most of starting materials. Compound **2** was formed in less than 5% yield. We reasoned the low yield might be due to the weak nucleophile of 3-amino-5-F pyridine and thus slow imine formation. Instead, a stepwise UGI reaction was conducted under more forcing conditions to prepare imine 4 (step d, **Scheme 1**). Then the resulting imine **4** reacted with acid and isocyanide to afford the intermediate **2**, following with a Buchwald-Hartwig reaction and diastereomers separation to afford the desired target compound **1b** (*S,S'*) and **1b'** (*S, R'*). In our in-house biochemical assay, the (*S, S*) diastereomer (IDH1^{R132H} IC_{50} for compound **1b** and **5a** was 94 nM and 85 nM respectively) are more potent than the (*S, R*) diastereomer (IDH1^{R132H} IC_{50} for compound **1b'** and **5a'**was both >10 000 nM).

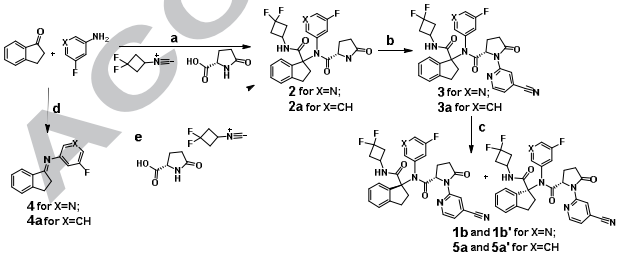

Scheme 1. General synthetic route of indane analogues. Reagents and conditions: (a) anhydrous MeOH, rt, overnight, <5% yield; (b)Cs_2CO_3, $Pd_2(dba)_3$, XantPhos, anhydrous 1,4-dioxane, N_2, 80°C, sealed tube, 3h, 50-72%; (c) diastereomers separation; (d) $ClCH_2CH_2Cl$, 4 Å MS, N_2, 5% $TiCl_4$, reflux, 12h; (e) anhydrous MeOH, rt, overnight, 30-50%.

From the docking model (**Figure 2-a**), compound **1b** overlayed well with AG120 in the same allosteric pocket in mutant IDH1^{R132H} crystal structure (PDB ID: 5tqh). [11] These two molecules were stabilized by two critical hydrogen bonds (HB), formed by its two terminal carbonyl groups with Tyr^{272} and Ala^{111}. Additional two HBs were formed by the cyano pyridine with the main chain NH of Leu^{120} and Ile^{128}. These four HBs provided key interactions for binding. The indane moiety formed π-π stacking with the indole ring of Trp^{267} and hydrophobic interactions with Val^{255}, Ala^{258} and Met^{259}. Further, the docking model suggested that compound **1a** or compound **1c** was less favored than compound **1b**, proved by the 3-fold decrease in enzymatic potency for **1a** and **1c** (**Table 1**). However, loss of two hydrogen bonds between compound **1b'**(*S, R*) and the protein resulted in a dramatic decrease of enzymatic potency (**Figure 2-b**).

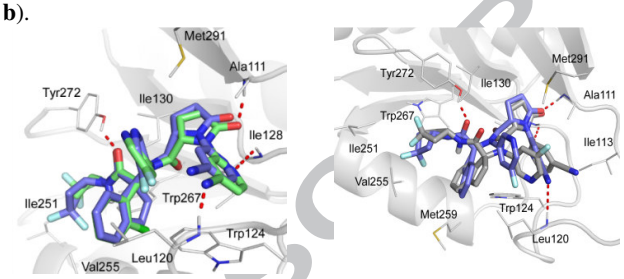

2-a 2-b

Figure 2. Superimposition of the putative binding modes for compounds. 2-a, binding mode for compound **1b** (blue sticks) and AG120 (green sticks) with IDH1^{R132H}; 2-b, binding mode for compound **1b** (blue sticks) and **1b'** (gray sticks) bound to mutant IDH1^{R132H}.

Since the activities between analog **1b** (X = N) and **5a** (X = CH) were quite similar (**Table 2**), we focused on the SAR exploration on analogs with X = CH due to their synthetic feasibility. In continuation with SAR studies, we first explored the top left side chain R group modification using a variety of cycles (**Table 2**). Replacement of 4-membered ring with 6-membered ring (**5b**) led to slight improvement in potency. The smaller cyclopropyl methyl analogue (**5c**) decreased potency by three fold. Interestingly, replacement of CH_2(compound **5e**) with O in the cyclohexyl group of compound **5d** caused loss of almost all the activity, which indicated that the hydrophilicity of R group might be unfavorable to the protein interaction. Similarly, rigid phenyl ring replacement (compound **5f**) was also unfavorable to the interaction.

Table 2. Enzymatic inhibition and 2-HG production inhibition activities in HT1080 for compound **1b** and **5a**-**5f**.

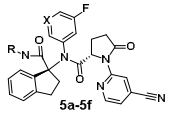

Cmpd	R	X	IDH1^{R132H} IC_{50}(nM)	2-HG HT1080 [a] IC_{50}(nM)
1b		N	94	21
5a		CH	85	25
5b		CH	80	15
5c		CH	266	NT

5d		CH	37	<10
5e		CH	>1000	NT
5f		CH	>1000	NT

Therefore compound **5a**, **5b** and **5d** were subjected to microsomal stability test. As shown in **Table 3**, the geminal di-F substitution in compound **5b** could significantly improve the metabbolitic stability of compound **5d**. The geminal di-F substituted cyclobutyl group (compound **5a**) could be further metabolic more stable and have slower turnover rate than compound **5d**. Hence gem di-F cyclobutyl group was fixed for further lead optimization.

Table 3. Mice, rat and human microsomal stabilities of compound **5a**, **5b** and **5d.**

Cmpd	Clint in vitro(mL/min/g protein)		
	Mouse	Rat	Human
5a	54.1	3.7	3.1
5b	567	24	35
5d	2359	1145	1005

With the fixed left side chain, substitutions on top benzene (R^1) were screened in **Table 4**. Removal of 3-F group (compound **6a**) from compound **5a** or replacement of 3-F group with 3-Cl (compound **6b**) both resulted in a 3-fold decrease of enzymatic potency. Then another fluorine was added to the different position in the phenyl ring of compound **5a** resulted in compound **6c**-**6f**. Interestingly, 3, 5-di fluorine analogue(**6f**) demonstrated improved enzymatic and cellular potency (45 nM and 5 nM respectively) and only 3, 4- di fluorine analogue (**6e**) could retain the enzymatic activity of compound **5a**, while 2,4-difluorine (compound **6c**) and 2,3-difluorineanalogues (**6d**) were 2-3 fold less potent than compound **5a**. As observed in above, the corresponding Cl substitution was not as effective as fluorine analogue (**6g** *vs* **6f**, **6h** *vs* **6e**). These results suggested that the *meta*-fluorine atom might have some hydrophobic interaction with the hydrophobic pocket consisted of the Leu^{120} and Trp^{124} side chains.

Table 4. Enzymatic inhibition and 2-HG production inhibition activities in HT1080 for compound **5a** and **6a**-**6h**.

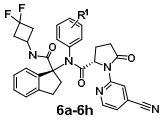

Cmpd		$IDH1^{R132H}$ IC_{50}(nM)	2-HG HT1080 [a] IC_{50}(nM)
5a		85	25
6a		260	NT
6b		255	NT
6c		338	NT
6d		148	NT
6e		95	NT
6f		45	5
6g		172	NT
6h		186	NT

The SAR for F or Cl substituted indane scaffold was also explored (**Table 5**). When fluorine atom was introduced at 4-, 5-, 6-, or 7-position to indane, the potency of compound **7a** and **7d** was slightly better than that of compound **7b** and **7c**. Fluorine at 4- or 7-position seemed to produce additional hydrophobic interaction based on docking model. Then larger Cl atom was installed at 4- or 7-position to indane ring system (**7e** and **7f**), which led to improved cellular activity (**7e** and **7f**, 21 nM and 7.5 nM respectively). To our surprise, when R^1 is F, only 4-Cl indane analogue could keep the inhibition potency of $IDH1^{R132H}$, while 7-Cl indane analogue lost 2 fold of its potency.

Table 5. Enzymatic inhibition and 2-HG production inhibition activities in HT1080 for compound **5a** and **7a**-**7h**.

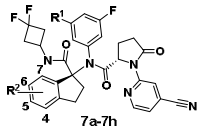

Cmpd	R^1	R^2	$IDH1^{R132H}$ IC_{50}(nM)	2-HG HT1080 [a] IC_{50}(nM)
5a	H	H	85	25
7a	H	4-F	68	27
7b	H	5-F	108	NT
7c	H	6-F	138	NT
7d	H	7-F	51	52
7e	H	4-Cl	67	21
7f	H	7-Cl	49	7.5
7g	F	4-Cl	53	14
7h	F	7-Cl	180	NT

After elucidated the SAR at three regions of this scaffold, we continued to expand the exploration on oxoproline group. According to the data from **Table 6**, the *R* isomer (**8a**) dramatically decreased its potency and proline analogue (compound **8b**) also lost most of its potency due to loss of the hydrogen bond with Ala^{111}. Interestingly, the carbamate analogue (compound **8c**) exhibited a little improvement in enzymatic potency.

Table 6. Enzymatic inhibition and 2-HG production inhibition activities in HT1080 for compound **5a** and **8a**-**8c**.

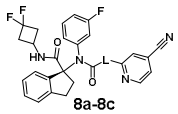

8a-8c

Cmpd	L	IDH1^{R132H} IC$_{50}$(nM)	2-HG HT1080 [a] IC$_{50}$(nM)
5a		85	25
8a		>10000	NT
8b		635	NT
8c		58	19

Finally, the bottom right R^3 group was investigated (**Table 7**). Based on the docking model, the N atom on pyridine interacted with the Ile[128] residue through hydrogen bond. In consistent with this hypothesis, 60-fold potency decrease was observed with the phenyl replacement (**9a**). The CN group (**9b**) was also crucial to potency (**9b**). Different substitution was thus designed to mimic this CN group. Pyrazine analogue (**9c**) decreased potency by two fold (128 nM), while the analogues with methoxyl group (**9d**) or methyl sulfonyl group (**9e**) were almost inactive. Pyrimidine nitrile compound **9f** improved the enzymatic potency by two fold (22 nM), but reduced the cellular activity by three fold (14.9 nM) possibly due to its poor physical and chemical property of aminopyrimidinyl group.

Table 7. Enzymatic inhibition and 2-HG production inhibition activities in HT1080 for compound **6f** and **9a**-**9f**.

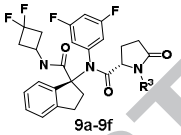

9a-9f

Cmpd	R^3	IDH1^{R132H} IC$_{50}$(nM)	2-HG HT1080 [a] IC$_{50}$(nM)
6f		45	5
9a		1. 2605	2. NT
3. **9b**	4. 	>10000	NT
9c		4.1.1. 128	4.1.2. NT
4.1.3. **9d**	4.1.4. 	4.1.4.1. >10000	4.1.4.2. NT
4.1.4.3. **9e**	4.1.4.4. 	4.1.4.4.1. 2965	4.1.4.4.2. NT
4.1.4.4.3. **9f**	4.1.4.4.4. 	22	14.9

We further attempted to combine all optimized structural features from different part of molecular into one compound (**10a**-**10e**, **Table 8**). Compound **10a** and **10b** retained enzymatic and cellular potency, while compound **10c** and **10d** resulted in decreased activity in cellular potency. Interestingly, compound **10e** demonstrated excellent enzymatic potency (5.6 nM, 9-fold and 15-fold improvement in comparison with that of compound **6f** and **1b**, respectively), but disappointedly did not transfer to more active cellular potency (29 nM in HT1080). We postulated that the lower permeability associated with the higher tPSA value in this compound might produce this result.

Table 8. Enzymatic inhibition and 2-HG production inhibition activities in HT1080 for compound **6f**, **7f** and **10a**-**10e**.

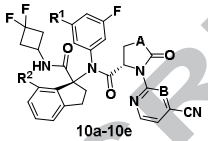

10a-10e

Cmpd	R^1	R^2	A	B	IDH1^{R132H} IC$_{50}$(nM)	2-HG HT1080 [a] IC$_{50}$(nM)	tPSA
6f	F	H	CH_2	CH	45	5	106
7f	H	Cl	CH_2	CH	49	7.5	106
10a	F	H	O	CH	54	8.9	115
10b	H	Cl	O	CH	42	9	115
10c	H	Cl	CH_2	N	22	42	118
10d	F	H	O	N	40	308	127
10e	H	Cl	O	N	5.6	29	127

To our delight, compound **6f** and **7f** with excellent cellular potency (IC_{50}<10 nM) also showed moderate to high selectivity against wild type IDH1 (79 and 36 fold respectively) and mutant IDH2^{R140Q} (>2000 fold) (**Table 9**). These two compounds were also progressed into primary mice pharmacokinetic (PK) study. Good PK parameters were observed with low clearance (<1.5 L/h/Kg) and high bioavailability (>30%) in mice (**Table 10**). It indicated that these two selected compounds might have good in vivo efficacy in nude mice.

Table 9. Selectivity of compound **6f** and **7f** against IDH1^{wt} and mutant IDH2.

Cmpd	IDH1^{R132H} IC$_{50}$(nM)	IDH1^{wt} IC$_{50}$(nM)	IDH2^{R140Q} IC$_{50}$(nM)	IDH1^{wt}/IDH1^{R132H}	IDH2^{R140Q}/IDH1^{R132H}
6f	45	3560	>100	79 fold	>2200 fold
7f	49	1780	>100	36 fold	>2040 fold

Table 10. Mouse PK parameters of compound **6f** and **7f**

Cmpd	Cl(L/hr/Kg) (iv, 1 mpk)	Vss (L)	AUC(ng/mL.hr) (iv, 1mpk)	AUC(ng/mL.hr) (po,5mpk)	F(%)
6f	0.5	1	1984	3620	87
7f	1.2	1.9	834	3780	38

iv formulation: 5%DMSO/95% saline; po formulation: 0.4%MC in deionized water.

In summary, a novel class of conformationally restricted indane analogues for IDH1 inhibitors were discovered and optimized *via*

structure-based rational design. The most advanced analogues **6f** and **7f** showed potent enzymatic and cellular activities, favorable mouse PK properties and great selectivity against wide-type IDH1 and mutant IDH2. These promising results strongly supported further development of these compounds into orally selective mutant IDH1 lead compounds.

Acknowledgements

This work was supported by the China International Science and Technology Cooperation Program (No. 2015DFM30040 to MH) and a grant from the National Natural Science Foundation of China (No. 81573464 to MH).

References and notes

1. (a) Zhou, K.G.; Jiang, L.J.; Shang, Z.; Wang, J.; Huang, L.; Zhou, J. Leukemia & Lymphoma, 2012, 53(12), 2423-2429. (b) Abbas S.; Lugthart, S.; Kavelaars, F.; Schelen, A; Koenders, J; Zeilemaker, A; van Putten Wim, J. L.; Rijneveld, A W; Lowenberg, B; Valk, P. J. M. Blood, 2010, 116(12), 2122-6. (c) Di Nardo, C. D.; Jabbour, E.; Ravandi, F.; Takahashi, K.; Daver, N.; Routbort, M.; Patel, K. P.; Brandt, M.; Pierce, S.; Kantarjian, H.; Garcia-Manero, G. Leukemia, 2016, 30(4), 980-984. (d) Paschka, Peter; Schlenk, R.F.; Gaidzik, V. I.; Habdank, M.; Kroenke, J.; Bullinger, L.; Spaeth, D.; Kayser, S.; Zucknick, M.; Goetze, K.; Horst, H.; Germing, U.; Doehner, H.; Doehner, K. J. Clin. Oncol. 2010, 28, 3636.
2. (a) Houillier, C.; Wang, X.; Kaloshi, G.; Mokhtari, K.; Guillevin, R.; Laffaire, J.; Paris, S.; Boisselier, B.; Idbaih, A.; Laigle-Donadey, F.; Hoang-Xuan, K.; Sanson, M.; Delattre, J-Y. Neurology, 2010, 75(17), 1560-1566. (b) Yan, H.; Parsons, D. W.; Jin, G.; McLendon, R.; Ahmed, R. B.; Yuan, W.S.; Kos, I.; Batinic-Haberle, I.; Jones, S.; Riggins, G. J.; Friedman, H.; Friedman, A.; Reardon, D.; Herndon, J.; Kinzler, K. W.; Velculescu, V.E.; Vogelstein, B.; Bigner, D. D. New Engl. J Med. 2009, 360(8), 765-773. (c) Parsons, D. W.; Jones, S.; Zhang, X.S.; Lin, J. C. H.; Leary, R. J.; Angenendt, P.; Mankoo, P.; Carter, H.; Siu, I.; Gallia, G. L.; Olivi, A.; McLendon, R.; Rasheed, B.; Keir, S.; Nikolskaya, T.; Nikolsky, Y.; Busam, D. A.; Tekleab, H.; Diaz, L. A.; Hartigan, J.; Smith, D.; Strausberg, R. ; Marie, S.; Kazue, N.; Shinjo, S.; Yan, H.; Riggins, G.; Bigner, D.; Karchin, R.; Papadopoulos, N.; Parmigiani, G.; Vogelstein, B.; Velculescu, V.; Kinzler, K. Science, 2008, 321, 1807.
3. Saha, S.K.; Parachoniak, C.A.; Ghanta, K. S.; Fitamant, J.; Ross, K.N.; Najem, M.S.; Gurumurthy, S.; Deshpande, V.; Zhu, A. X.; Ferrone, C.R.; Bardeesy, N.; Akbay, E.A.; Wong, K-K.; Sia, D.; Cornella, H.; Miltiadous, O.; Walesky, C.; Apte, U.; Hezel, A.F.; Yen, K.E.; Straley, K.S.; Travins, J.; Popovici-Muller, J.; Gliser, C.; Llovet, J.M.;Ramaswamy, S. K. Nature, 2014, 513,110–114.
4. Amary M.F.;, Bacsi K.; Maggiani F.; Damato S.; Halai D.; Berisha F.; Pollock R.; O'Donnell P.; Grigoriadis A.; Diss T.; Eskandarpour M.; Presneau N.; Hogendoorn P.C.; Futreal A.; Tirabosco R.; Flanagan A.M. J Pathol., 2011, 224(3), 334–343.
5. Kang, M. R; Kim, M.; Oh, J.; Kim, Y; Song, S.; Seo, S.; Lee, J.; Yoo, N.; Lee, S. Int J Cancer,2009, 125(2), 353-355.
6. Reitman Z.J., Parsons D.W., Yan H. Cancer Cell, 2010, 17, 215–216.
7. Chaturvedi, A.; Cruz, M.; Jyotsana, N.; Sharma, A.; Yun, H.; Goerlich, K.; Wichmann, M.; Schwarzer, A.; Preller, M.; Thol, F.; Meyer, J.; Haemmerle, R.; Struys, E.A.; Jansen, E.; Modlich, U.; Li, Z; Sly, L.; Geffers, R.; Lindner, R.; Manstein, D.; Lehmann, U; Krauter, J; Ganser, A.; Heuser, M. Blood, 2013, 122, 2877–87.
8. http://investor.agios.com/phoenix.zhtml?c=251862&p=irol-newsArticle&ID=2227727.
9. Dömling, A.; Ugi, I. Angew. Chem.-Int. Edit. 2000, 39, 3168–3210.
10. Lemieux, Rene M.; Poovici-muler, Janeta et al. WO2013107291A1.
11. Levell J.R.;Caferro T.;Chenail G.;Dix I.;Dooley J.; Firestone B.;Fortin P.D.;Giraldes J.;Gould T.;Growney J.D.;Jones M.D.;Kulathila R.;Lin F.;Liu G.;Mueller A.;van der Plas S.;Slocum K.;Smith T.;Terranova R.;Touré B.B.;Tyagi V.;Wagner T.;Xie X.;Xu M.;Yang F.S.;Zhou L.X.;Pagliarini R.;Cho Y.S. ACS Med. Chem. Lett., 2016,8(2),151-156.
12. All synthesized compounds in this article were characterized by HNMR and LCMS. Their purity was at least 95% for the enzymatic and cellular assay and 98% for mouse PK study.

Supplementary Material

Chemistry, biological assay information and docking method. This material is available free of charge via the internet.